 doi.org/10.52568/001460/JCSP/46.03.2024

Effect of Fabricated Nanostructure on Biological Activity of Synthesized Benzamide Cationic Surfactants

[1,2]Eid M. S. Azzam*, [2]Abdallah R. Ismail, [1]Khalaf M. Alenezi, [1]Hani El Moll
[1]Lassaad Mechi, and [1,3]Walaa I. El-sofany
[1]*Department of Chemistry, College of Sciences, University of Ha'il, Ha'il 81451, Kingdom of Saudi Arabia.*
[2]*Egyptian Petroleum Research Institute, Nasr City, 11727 Cairo, Egypt.*
[3]*Photochemistry Department, Chemical Industries Research Institute, National Research Centre, Scopus affiliation ID 60014618, 33 EL Buhouth St., Dokki, Giza 12622, Egypt.*
eazzamep@yahoo.com*

(Received on 6th April 2023, accepted in revised form 13th February 2024)

Summary: Nanomaterials, such as Ag-nanoparticles (AgNPs), have recently been shown to have a broad range of applications in the chemical industry, medicine, biology, and many areas. In this work, the effect of nanostructure on the biological efficiency of prepared surfactants (R10, R12) based on the benzamide group was reported. FTIR and ^{1}HNMR spectra were collected to confirm the structure of these surfactants. In addition, the nanostructures of the prepared surfactants assembled on Ag-nanoparticles (AgNPs) were investigated using UV and TEM techniques. Moreover, the antimicrobial properties of the prepared surfactants and their associated nanostructures were studied. The results showed that, with the exception of Pseudomonas aeruginosa and Escherichia coli, the antibacterial effectiveness of R12AgNPs against all bacteria was better than R12. In contrast, the antibacterial activity of R10AgNPs against all bacteria was lower than R10. This might be explained by the fact that AgNPs were effective on the manufactured surfactant's CMC (R10), which decreased the amount of surfactant molecules at the cell membrane and decreased the antibacterial activity. The outcomes showed that the cationic surfactants (R10, R12) that were synthesized favored AgNP dispersion and enhanced their activity.

Keywords: Benzamide, Cationic surfactants, Ag-nanoparticles, Nanostructure, Antimicrobial activity.

Introduction

Nanomaterials are a subclass of materials that have an extraordinary surface and at least one dimension with an average size of 1 to 100 nm. Special structures, high surface-to-volume ratio and a large number of atoms residing on their surfaces have distinguished nanomaterials. The properties of bulk materials can improve or be created by engineered nanomaterials in terms of strength , conductivity , catalytic, antibacterial properties, etc. [1-3]. Cationic surfactants have broad used as antimicrobial agents in many fields [4]. Cationic surfactants are different from the traditional antibiotics, which depend on a 'key & lock' mechanism involving attacking on microbial cells by hydrophobic and electrostatic interactions [5, 6]. The alkyl chain (hydrophobic part) and positive charge in the hydrophilic part of a surfactant are important factors determining their antimicrobial activity. The cytotoxicity of such surfactants is also dominant. Some modifications have been made to the structure of cationic surfactants to prepare low-toxicity antimicrobial surfactants recently. For example, it has been found that the integration of certain bioactive groups, such as amino acids [7], amides [5], or cyclodextrin [5] evidently reduce surfactant cytotoxicity [8]. In addition, the charge density affects the ability of a surfactant to act as an antimicrobial agent. Two main structural factors play a urgent role in the potential of the cationic surfactant: the first the counter-anions and the cationic head group, while the second is the hydrophobic part of the cationic surfactant, which is directly affected by the length, number and nature of the alkyl chain [4]. The importance of AgNPs is related to their exhibiting a consistent number of flexible properties, which lead to their large spectrum of applications in biomedicine and related fields [9]. Many research papers utilizing AgNPs as an antimicrobial agent [10]. The antibacterial effect of Ag-nanoparticles is dose-dependent and independent of the acquisition of resistance by bacteria against antibiotics [11]. The antibacterial efficiency of the surfactants in this work against sulphate-reducing bacteria (SRB) have discussed [12], which play interesting roles in increase the corrosion of pipelines in the petroleum field [13]. Our new target in this research is clarify the biological role of the prepared surfactants (R10 and R12) and the effect of their nanostructure (including AgNPs) towards Gram-(+ev) bacteria, Gram-(-ev) bacteria, yeast, and fungi.

Experimental

Synthesis of surfactants (R10 and R12)

The cationic surfactants R10 and R12 were synthesized as follows: 4-amino pyridine (9.4 g, 0.1 mol.)

*To whom all correspondence should be addressed.

was added to 4-amino benzoic acid (13.7 g, 0.1 mol.) using 50 mL of xylene as a solvent with few drops of sulphuric acid. Then refluxing until produced 1.8 ml of water which indicated the condensation reaction between the NH_2 and COOH group. The yield was collected after evaporation of the solvent. Then, the 4-amino-N-(pyridine-4-yl) benzamide and equal moles of decyl bromide or dodecyl bromide were refluxed in 50 mL of absolute ethanol for 50 h. The yield products of the prepared surfactants (R10, R12) were purified and recrystallized using diethyl ether and ethanol, respectively [12]. The structure of these surfactants in Scheme 1 was confirmed using FTIR and ^{1}HNMR.

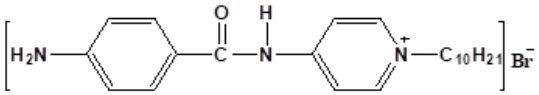

p-amino-N-((1-decylpyridin-1-ium bromide)-4-yl) benzamide (R10)

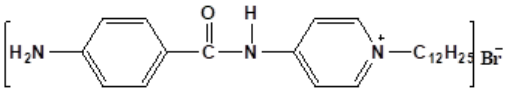

p-amino-N-((1-dodecylpyridin-1-ium bromide)-4-yl) benzamide (R12)

Scheme-1: The synthesized surfactants (R10 and R12).

Ag-nanoparticles colloidal solution (AgNPs)

The AgNPs solution was prepared, according to the following method detailed in the previous publication [12]. Trisodium citrate aqueous solution (5 ml, 1 %) was added to an aqueous solution of $AgNO_3$ (50 ml, 10^{-3} M). Then, it was vigorously stirred and boiled until the colour converted from colourless to pale yellow.

Fabricated nanostructure of R10 and R12 surfactants.

The AgNPs (prepared in step 2.2) was uesd for fabrication of the nanostructure of R10 and R12 surfactants as follows: The R10 or R12 compound was dissolved in deionized water (5 ml) and added to 20 ml of the prepared AgNPs. The solution was stirred vigorously for 24 hours, until disappearance of the yellow colour [12].

Antimicrobial Effect of R10 and R12

Antimicrobial effect and Minimum inhibitory concentration (MIC) assays for the prepared cationic surfactants (R10, R12) with/without Ag-nanoparticles were performed using the agar-well diffusion method [13]. Six microbes were used for the antimicrobial activity assay: Gram-(+ev)bacteria (*Bacillus subtilis* ATCC 6633 and *Staphylococcus aureus* ATCC 35556), Gram-negative bacteria (*Escherichia coli* ATCC 23282 and *Pseudomonas aeruginosa* ATCC 10145), Yeast (*Candida albicans* IMRU 3669), and Filamentous Fungus (*Aspergillus niger* ATCC 16404). Nutrient agar, Wickerham, and Potato dextrose agar media were prepared for the bacteria (Gram-(+ev) and Gram-negative), yeast, and fungus, respectively. The prepared media were autoclaved at 121 ^{o}C for 20 min, then injected with the previously 24 h-cultivated tested microbes, and immediately poured into 90 mm Petri-dishes before solidification. Six wells (8 mm in diameter) were designed using a cork borer on the agar plate. Then, 100 µl of the homogenized tested compounds at 5 mg ml^{-1} concentration was injected into each agar-well. The samples were kept for 24 h and 48 h at 37 ^{o}C and 30 ^{o}C for bacteria and yeast/fungus, respectively. For the MIC test, two-fold serial dilutions were applied to the initial concentration of the tested compounds (5 mg ml^{-1}). *Streptomycin* (0.1 mg ml^{-1}) as an antibacterial, *Nalidixic* acid (0.1 mg ml^{-1}) as an antiyeast, and *Fluconazole* (0.1 mg ml^{-1}) as an antifungal were utilized as positive controls. All methods were repeated in triplicate, and the results are presented as mean ± SD.

Results and Discussion

Structure of the prepared surfactants (R10, R12)

The FTIR spectroscopy (Fig. 1) and ^{1}H-NMR spectra (Fig. 2) were conducted to confirm the structure of the R10 and R12. The FTIR spectrum of R10 surfactant presented adsorption bands of the synthesized surfactants as observed in the previous publication [12] at 2853 cm^{-1} (CH_3 and sym. CH_2 stretch.), 2924 cm^{-1} (asym. CH_2 stretch.), and 1381 cm^{-1} (CH_2 bend.). Bands also appeared at 1468 cm^{-1} (aromatic C=C stretch.), 1176 cm^{-1} (C–N stretching), 3153 cm^{-1} (N–H stretch, amide), 3312 cm^{-1} (N–H stretch., amine), 1656 cm^{-1} (NH_2 bend., amine), and 1600 cm^{-1} (C=O stretch., amide). Meanwhile, the FTIR spectrum for compound R12 presented adsorption bands at 2976 cm^{-1} (CH_2 stretch.), 1381 cm^{-1} (CH_2 bend.), 1530 cm^{-1} (Ar. C=C stretching), 1176 cm^{-1} (C–N stretch.), 3153.2 cm^{-1} (N–H stretch., amide), 3312 cm^{-1} (N–H stretch., amine), 1656 cm^{-1} (NH_2 bend., amine), and 1600 cm^{-1} (C=O stretch., amide). The difference in the band positions between R10 and R12 surfactants was due to the chain length effect. The ^{1}H-NMR spectra for R10 and R12 presented the peaks of different groups, as discussed in previous publication [12]. The ^{1}H-NMR spectra for R10 presented bands at 0.86–0.83 ppm (t, 3H, CH_3,), 1.23 ppm (m, 14H, CH_2),

1.67–1.70 ppm (q, 2H, beta CH_2), and 2.51 ppm (s, 2H, NH_2, amine), in addition to bands at 3.02–4.14 ppm (t, 2H, N–CH_2), 8.21–8.19 ppm (d, 2H, pyridine), 8.13–8.21 ppm (d, 2H, pyridine), 6.54–6.56 ppm (d, 2H, Ar.), 6.58–6.57 ppm (d, 2H, Ar.), 6.60–6.63 ppm (d, 2H, Ar.), 6.65 (d, 2H, Ar.), and 13.03 ppm (s, H, NH, amide). Furthermore, the ^{1}H NMR spectra of compound R12 presented bands for CH_2 and CH_3 at δ = 0.83–0.86 ppm (t, 3H, CH_3), 1.23 ppm (m, 16H, CH_2), 1.53–1.74 ppm (q, 2H, beta CH_2), and 2.51 ppm (s, 2H, NH_2, amine), as well as other bands appearing at 3.02–4.12 ppm (t, 2H, N–CH_2), 8.21–8.19 ppm (d, 2H, pyridine), 8.12–8.11 ppm (d, 2H, pyridine), 7.63–7.61 ppm (d, 2H, Ar.), 6.84–6.83 ppm (d, 2H, Ar.), 6.81–6.58 (d, 2H, Ar.), 6.56–6.53 (d, 2H, Ar.), and 13.03 ppm (s, H, NH, amide).

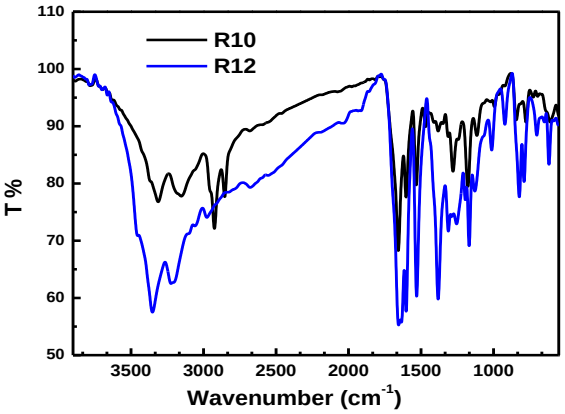

Fig. 1: FTIR spectrum of the prepared compounds R10 and R12.

Nanostructure of the surfactant capped AgNPs

We used an Evolution™ 300 UV-Vis spectrophotometer in the wavelength range of 200–800 nm at room temperature to investigate the prepared solution of the individual AgNPs and the solutions of Ag-nanoparticles with R10 and R12 surfactants [10]. The absorbance spectra of AgNPs before and after the addition of R10 and R12 surfactants are presented in Fig. 3. The absorbance peak for AgNPs shown at about 427 nm is due to the surface plasmon absorption of silver clusters [13]. Due to the capping of R10 and R12 on the AgNPs, new peaks appeared at about 265 nm and 271 nm, respectively (Fig. 3), due to the capping of surfactants on AgNPs displacing silver ions from the AgNPs and reducing their charge. Therefore, the frequency of collisions was increased [13]. The nanostructure of the prepared AgNPs and AgNPs with the synthesized cationic surfactants (R10 and R12) was analysed using a TEM (model JEOL JeM – 2100, Japan) [10]. Fig. 4 presents the TEM micrographs of the individual AgNPs solution and the AgNPs in the presence of surfactants R10 and R12. The nanostructure of AgNPs in the figure can be seen to take a spherical shape and polycrystalline structure, with size (20.9–34 nm). After capping the surfactant molecules on the AgNPs, nanoshells were formed, leading to reduction in the size by about 4.63–9.92 and 1.73–2.79 nm for the R10 and R12 (Fig. 4). In addition, the assembling of R10 and R12 molecules increased the stability of the AgNPs and reduced their aggregation. Therefore, the increase in surfactant chain length enhances the stabilization of AgNPs. It has been concluded, in a previous publication [13], that the alkyl chain length which provides a physical barrier preventing aggregation between the surfaces of AgNPs during collisions, in addition to the effect of surfactant molecules on the charge of AgNPs, that is, the R10 and R12 reduce the surface charge of the AgNPs. These factors led to an overall reduction in the aggregation of AgNPs.

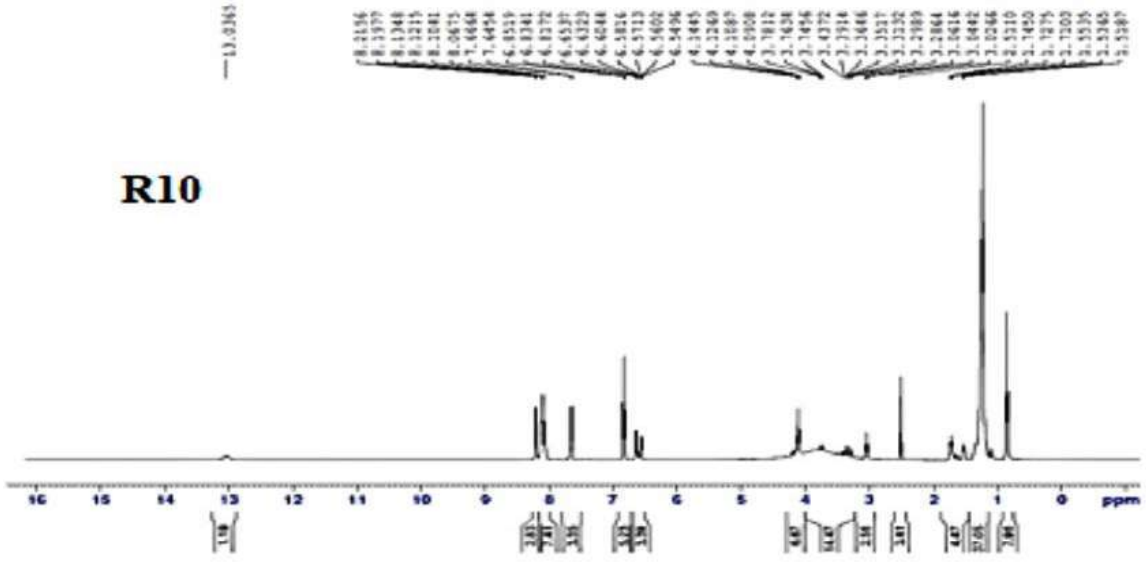

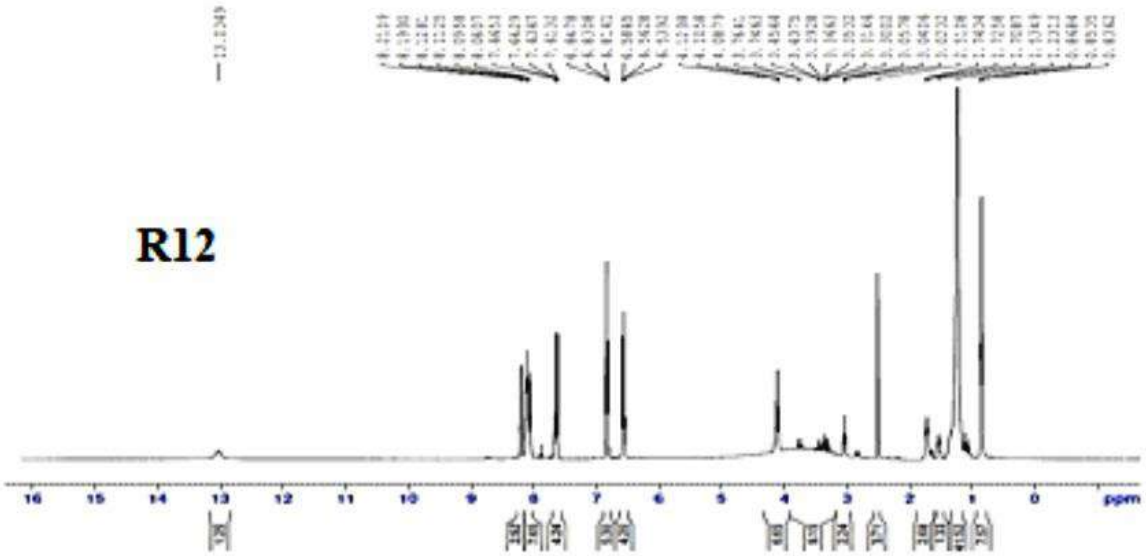

Fig. 2: [1]HNMR spectra of the prepared compounds R10 and R12.

Table-1: Antimicrobial activity (inhibition zone (mm)) of the prepared cationic surfactants and cationic surfactant capping AgNPs.

Compound ID	B. subtilis	S. aureus	E. coli	P. aeruginosa	C. albicans	A. niger
R10	40.1 ± 0.3	41.9 ± 0.2	21.9 ± 0.12	22.2 ± 0.16	40.8 ± 0.19	40.2 ± 0.22
R12	26.5 ± 0.1	26.9 ± 0.17	19.2. ± 0.1	18.7 ± 0.15	31.6 ± 0.18	30.6 ± 0.2
Ag	11.2 ± 0.1	11.5 ± 0.13	11.2 ± 0.12	11.1 ± 0.1	13.8 ± 0.12	13.4 ± 0.18
R10 AgNPs	37.2 ± 0.2	37.8 ± 0.21	16.8 ± 0.16	16.6 ± 0.1	36.5 ± 0.2	36.8 ± 0.19
R12 AgNPs	28.6 ± 0.2	28.8 ± 0.15	15.9 ± 0.1	16.4 ± 0.12	35.6 ± 0.18	35.5 ± 0.16
Positive control	31.5 ± 0.12	32.68 ± 0.11	28.1 ± 0.11	27.9 ± 0.11	29.1 ± 0.13	30.2 ± 0.14

Effect of nanostructure on the antimicrobial activity

The R10, R12 and their solutions with AgNPs (R10AgNPs and R12AgNPs, respectively) were tested to detect their effective to inhibit the growth of different types of micro-organisms (Gram-(+ev), Gram-(-ev) bacteria, yeast, and fungi). For the prepared cationic surfactants, it was found that the antimicrobial activity depended mainly on the aliphatic chain length, this phenomenon is the cut-off effect phenomena [14, 15]. There are many parameters dependent upon the occurrence of the cut-off effect phenomenon, including critical micelle concentration (CMC) of the surfactant, the change in the free energy of adsorption of the cationic surfactant on the bacterial cell membrane, the hydrophobic property, and the size of the absorbed surfactant [13]. The optimal antimicrobial activity occurs in medium chain lengths cationic surfactants. While, surfactants with alkyl chain less than 4 or more than 18 are mostly inactive [16]. Moreover, in the medium chain length range, an increase in the surfactant's aliphatic chain length decreases the critical micelle concentration, thus lowering the surfactant concentration at the cell membrane. Accordingly, surfactant activity will be greater with a shorter chain length (i.e., R10 > R12). However, on the other hand, the adsorption capacity at the membrane interface should become greater when increasing the hydrophobicity of the surfactant. Gram--(-ev) bacteria are more antibiotic efficiency than Gram-(+ev) bacteria, yeast, and fungi. The external membrane which composed of lipopolysaccharide molecules and periplasmic space in the Gram-(-ev) bacterial cell prevent the penetration of antibacterial agents, which make it more antibiotic-resistant [17-19].

Our findings, as shown in Table-1, were in clear agreement with the previously mentioned phenomena, as the activity of R10 against Gram-(+ev) bacteria, yeast, and fungi was significantly higher than that of R12. Meanwhile, it was only slightly higher in the status of Gram--(-ev) bacteria, because of the resistance showed by Gram-(-ev) bacteria due to the effective of outer membrane and periplasmic space [4]. Generally, the results were good. It was found that Ag-nanoparticles capped with the cationic surfactants successfully affected microbial growth. After dispersion in these surfactants, the antibacterial behaviour for pure AgNPs was clearly improved. As

detailed in Table-1, the inhibition zones of the AgNPs were significantly increased, by more than two folds. It can be noted, from the results in

Table-1, that the antibacterial activity of R10AgNPs towards all bacteria was lower than R10, while the antibacterial efficiency of R12AgNPs against all bacteria was higher than R12, except for *Escherichia coli* and *Pseudomonas aeruginosa*. This may be attributed to the effective of AgNPs on the CMC of the prepared surfactant (R10), leading to a decrease in surfactant molecules at the cell membrane and lower antibacterial activity. The results indicated that the prepared cationic surfactants (R10, R12) favoured the dispersion of AgNPs and improved their biocompatibility. The inhibitory effect of capped AgNPs may be attributed to the generation of free radicals and ROS in microbial cells, leading to the disruption of cell membrane and damage of cellular proteins, as clear in Fig. 3 [20].

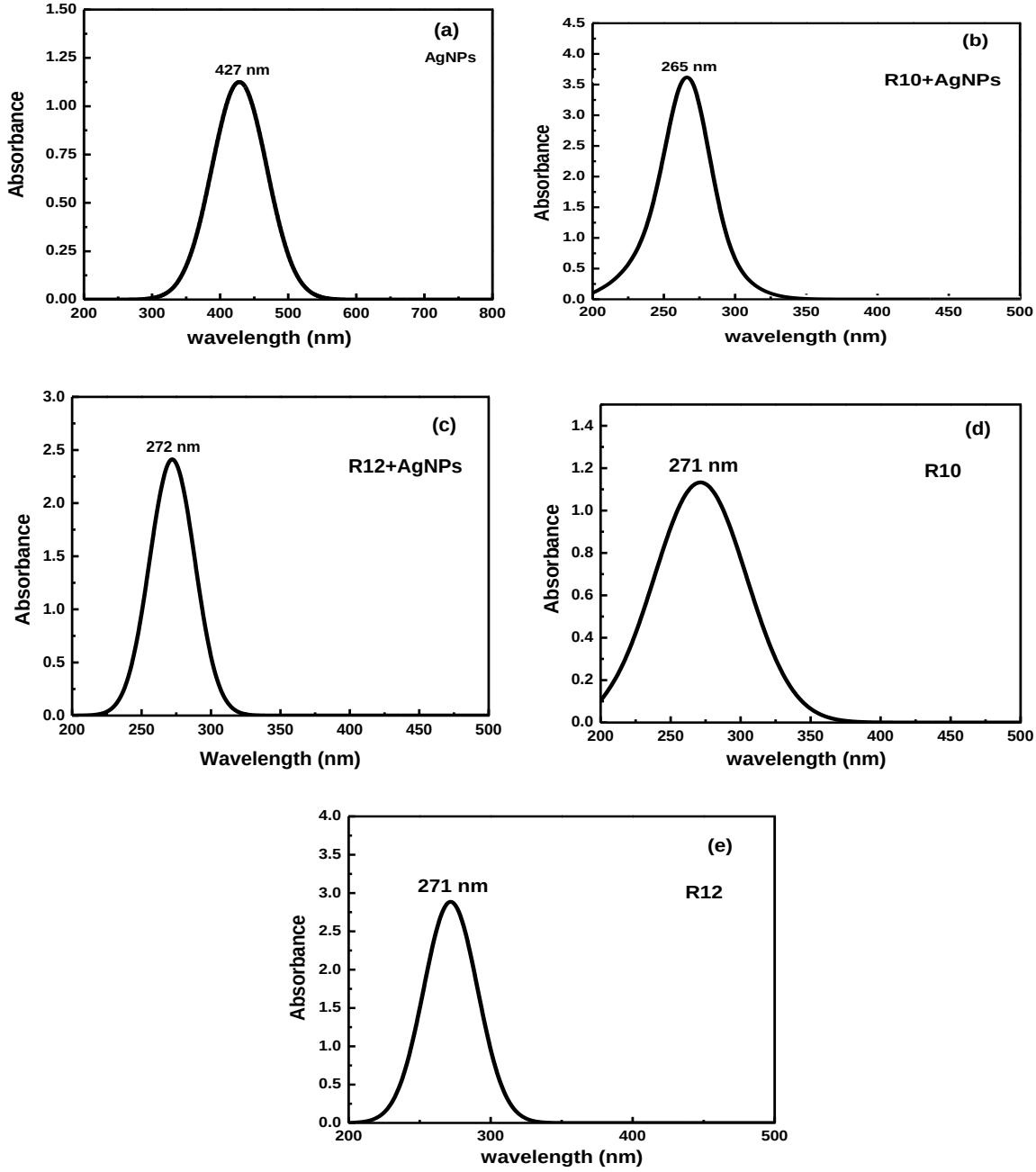

Fig. 3: UV spectra of: (a) The prepared AgNPs, (b) R10- and (c) R12-capped AgNPs, and (d) R10 and (e) R12.

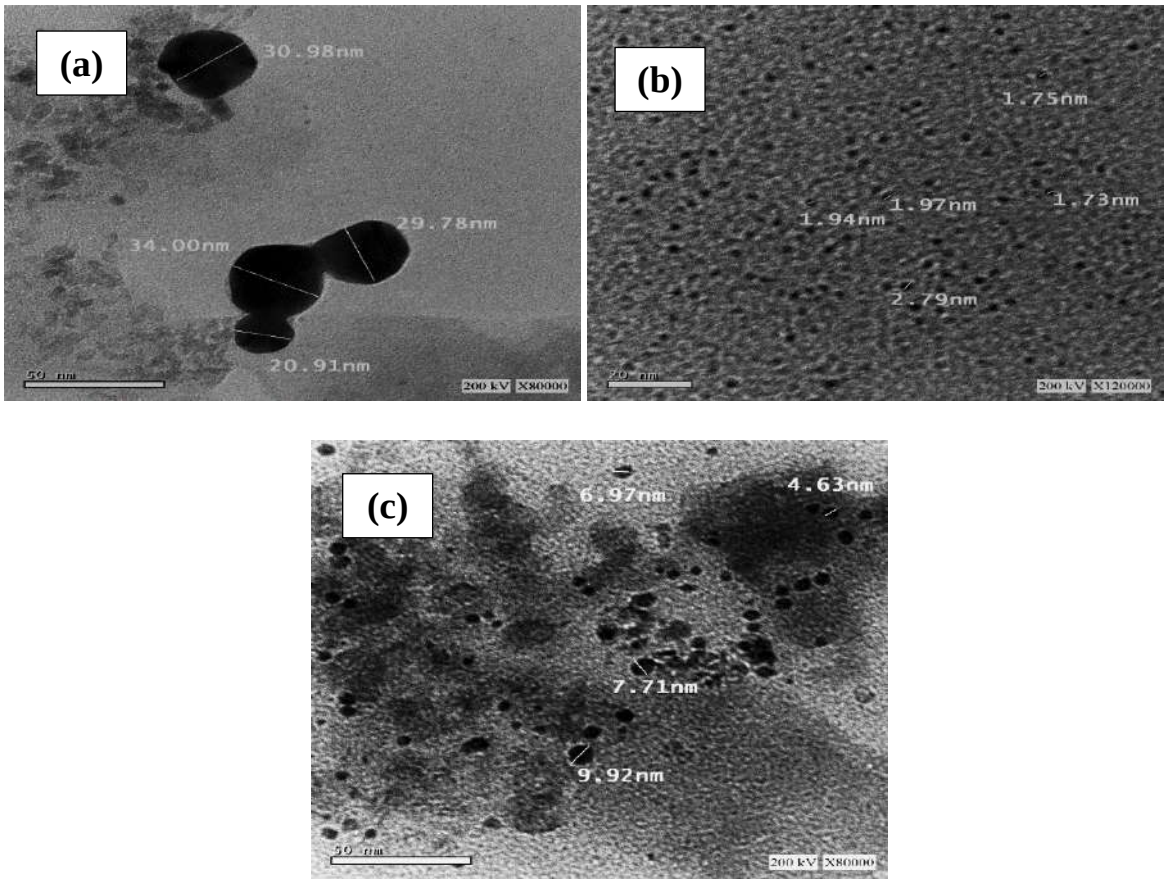

Fig. 4: TEM of: (a) The prepared AgNPs, and (b) R10- and (c) R12-capped AgNPs.

The minimum inhibition concentration (MIC) of the tested compounds (R10 and R12) and their associated nanostructures (R10AgNPs and R12AgNPs, respectively) were analysed using the agar-well diffusion method. The results listed in Table-2 indicate the minimum concentration of the tested compounds at which the inhibition of microbial growth was visible. The results in Table-2, clarify that there was a decrease in the MIC for the inhibition of microbial growth using the nanostructure of the prepared surfactants, especially for the R12 nanostructure. This is related to the above reasoning regarding the effect of AgNPs causing disruption to the cell membrane and damage of cellular proteins, as represented in Fig. 5 [20].

ANOVA analyzes the variation between groups in terms of the antimicrobial activity data.

The ANOVA data in Table-3 shows the sources of variation, including "Between Groups" and "Within Groups". The "Between Groups" variation represents the differences in antimicrobial activity among the different compounds tested. The "Within Groups" variation represents the differences within each group or compound. Table-3 provides the sum of squares (SS), degrees of freedom (df), mean squares (MS), F-value, p-value, and critical F-value (F crit). Based on the ANOVA data (Table-3), the p-value for the "Between Groups" variation is 0.000237, which is less than the significance level of 0.05. This indicates that there are significant differences in antimicrobial activity among the compounds tested. The F-value of 6.810904 suggests that there is a significant difference between groups. The F crit value of 2.533555 represents the critical F-value at a significance level of 0.05 and the given degrees of freedom.

Table-2: MIC (µg ml^{-1}) of the prepared cationic surfactants and cationic surfactant capping AgNPs.

Compound ID	*B. subtilis*	*S. aureus*	*E. coli*	*P. aeruginosa*	*C. albicans*	*A. niger*
R10	**78**	**78**	**156**	**156**	**78**	**78**
R12	**156**	**156**	**312**	**312**	**156**	**156**
R10 AgNPs	**78**	**78**	**312**	**312**	**78**	**78**
R12 AgNPs	**78**	**78**	**312**	**312**	**78**	**78**

Table-3: ANOVA analyzes the variation between groups in terms of the antimicrobial activity data.

ANOVA: Single Factor						
SUMMARY						
Groups	*Count*	*Sum*	*Average*	*Variance*		
R10	6	207.1	34.51667	93.66967		
R12	6	153.5	25.58333	30.41367		
Ag	6	72.2	12.03333	1.506667		
R10 AgNPs	6	181.7	30.28333	110.8977		
R12 AgNPs	6	160.8	26.8	77.468		
Positive control	6	179.48	29.91333	3.651467		
ANOVA						
Source of Variation	*SS*	*df*	*MS*	*F*	*P-value*	*F crit*
Between Groups	1802.66	5	360.532	6.810904	0.000237	2.533555
Within Groups	1588.036	30	52.93452			
Total	3390.696	35				

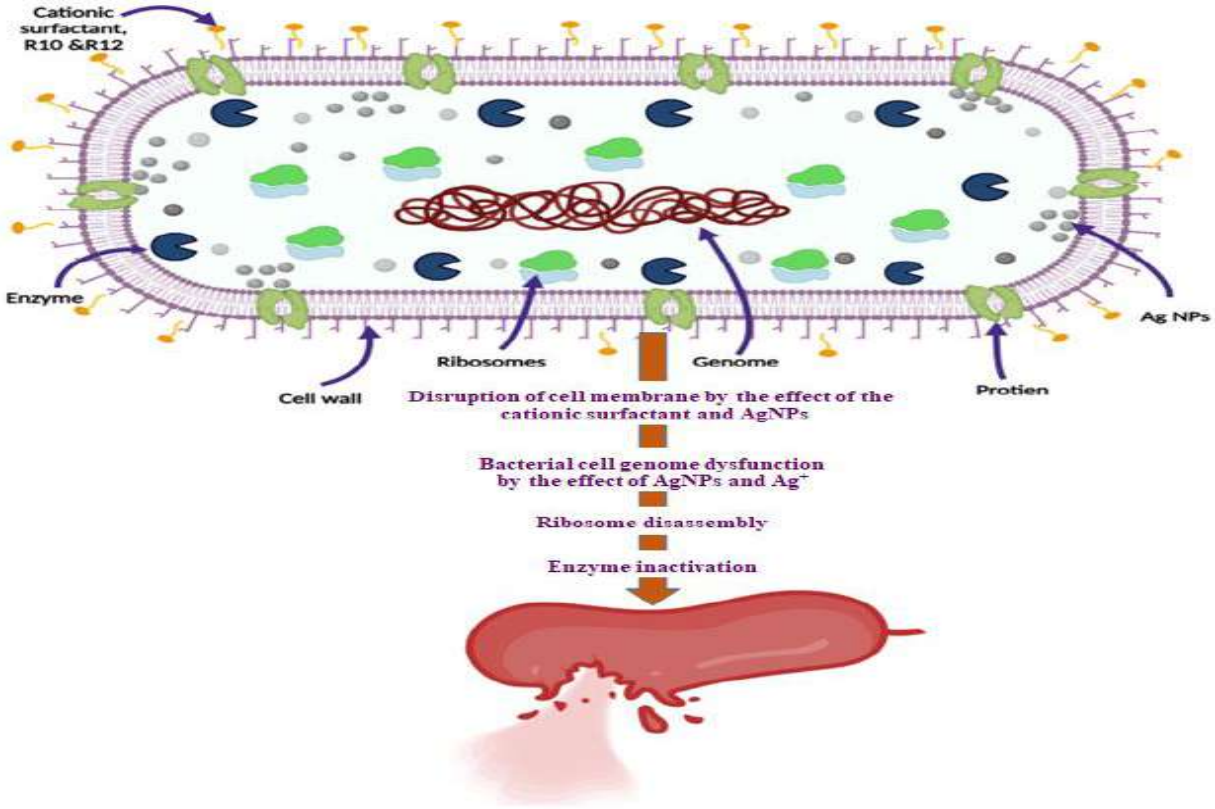

Fig. 5: Different modes of action of cationic surfactants (R10, R12) and AgNPs capped with cationic surfactants on the bacterial cell.

ANOVA analyzes the variation between groups in terms of the MIC data.

The ANOVA data in Table -4 provide that the p-value for the "Between Groups" variation is 0.34983, which is higher than the significance level of 0.05. This suggests that there are no significant differences in MIC among the compounds tested. Also, the F-value of 1.15942 indicates a relatively low level of variation between groups. Moreover, the F crit value of 3.098391 represents the critical F-value at a significance level of 0.05 and the given degrees of freedom.

In summary, the statistical data in the document provides information about the antimicrobial activity and MIC of different compounds against various microorganisms. The ANOVA results indicate significant differences in antimicrobial activity between the compounds, while the MIC data does not show significant differences.

Table-4: ANOVA analyzes the variation between groups in terms of the MIC data.

ANOVA: Single Factor						
SUMMARY						
Groups	***Count***	***Sum***	***Average***	***Variance***		
R10	**6**	**624**	**104**	**1622.4**		
R12	**6**	**1248**	**208**	**6489.6**		
R10 AgNPs	**6**	**936**	**156**	**14601.6**		
R12 AgNPs	**6**	**936**	**156**	**14601.6**		
ANOVA						
Source of Variation	***SS***	***df***	***MS***	***F***	***P-value***	***F crit***
Between Groups	**32448**	**3**	**10816**	**1.15942**	**0.34983**	**3.098391**
Within Groups	**186576**	**20**	**9328.8**			
Total	**219024**	**23**				

Conclusions

The antimicrobial activities of the R10 and R12 and their nanostructures based on AgNPs towards Gram-(+ev) and Gram-(-ev) bacteria, yeast, and fungi were investigated. Various techniques were used to study the capping of AgNPs by the R10 and R12, including UV and TEM. The prepared surfactants and their nanostructures with AgNPs presented good antimicrobial activity. It can be concluded that R10 and R10AgNPs have higher biological activity than R12 and R12AgNPs. In addition, the results of this work indicate the possibility for using of the R10, R12, R10AgNPs and R12AgNPs as biocides against bacteria, yeast, and fungi. It is clear from the ANOVA results that there is a significant differences in antimicrobial activity between the compounds R10 and R12, in contrast the MIC data does not show significant differences.

Acknowledgement

This research was funded by scientific research deanship at University of Ha'il, Saudi Arabia, through project number RG-21125.

References

1. Ramezani Farani, M., Farsadrooh, M., Zare, I., Gholami, A., & Akhavan, O. Green Synthesis of Magnesium Oxide Nanoparticles and Nanocomposites for Photocatalytic Antimicrobial, Antibiofilm and Antifungal Applications. *Catalysts*, **13**, 642 (2023).
2. Chouke, P. B., Shrirame, T., Potbhare, A. K., Mondal, A., Chaudhary, A. R., Mondal, S. & Chaudhary, R. G. Bioinspired metal/metal oxide nanoparticles: A road map to potential applications. *Materials Today Advances*, **16**, 100314 (2022).
3. Rahimnejad, M., Rasouli, F., Jahangiri, S., Ahmadi, S., Rabiee, N., Ramezani Farani, M. & Hahn, S. K., Engineered biomimetic membranes for organ-on-a-chip. *ACS Biomaterials Science & Engineering*, **8**, 5038 (2022).
4. C. Zhou and Y. Wang, Structure–activity relationship of cationic surfactants as antimicrobial agents, *Curr. Opin. Colloid In.*, **45**, 28 (2020).
5. J. Hoque, P. Akkapeddi, V.Yarlagadda, D. S. Uppu, P. Kumar and J. Haldar, Cleavable cationic antibacterial amphiphiles: synthesis, mechanism of action, and cytotoxicities, *Langmuir*, **28**, 12225 (2012).
6. J. Hoque, M. M. Konai, S. Samaddar, S. Gonuguntala, G. B. Manjunath, C. Ghosh, and J. Haldar, Selective and broad spectrum amphiphilic small molecules to combat bacterial resistance and eradicate biofilms, *Chem. Commun.*, **51**, 13670 (2015).
7. A. Pinazo, M. A. Manresa, A. M. Marques, M. Bustelo, M. J. Espuny, and L. Pérez, Amino acid–based surfactants: New antimicrobial agents, *Adv. Colloid Interfac.*, **228**, 17 (2016).
8. A. Colomer, A. Pinazo, M. A. Manresa, M. P. Vinardell, M. Mitjans, M. R. Infante, and L. Pérez, Cationic surfactants derived from lysine: effects of their structure and charge type on antimicrobial and hemolytic activities, *J. Med. Chem.*, **54**, 989 (2011).
9. K. Kalwar and D. Shan, Antimicrobial effect of silver nanoparticles (AgNPs) and their mechanism–a mini review, *Micro Nano Lette.* **13**, 277 (2018).
10. E. M. S. Azzam, A. El-Salam, and R. S. Aboad, Kinetic preparation and antibacterial activity of nanocrystalline poly (2-aminothiophenol), *Polym. Bull.*, **76**, 1929 (2019).
11. V. Arya, R. Komal, M. Kaur, and A. Goyal, Silver nanoparticles as a potent antimicrobial agent: a review, *Pharmacologyonline*, **3**, 118 (2011).
12. E. M. S. Azzam, R. M. Sami, K. M. Alenezi, A. Haque, H. El Moll, Soury R A, and A. R. Ismail, Inhibition of Sulfate-Reducing Bacteria by Para-amino-N-((1-Alkylpyridin-1-Ium Bromide)-4-Yl) Benzamide Surfactants and Surfactant-Coated Silver Nanoparticles, *J. Surfactants Deterg.*, **25** 125 (2022).
13. S. M. Shaban, I. Aiad, and A. R. Ismail, Surface parameters and biological activity of N-(3-

(dimethyl benzyl ammonio) propyl) alkanamide chloride cationic surfactants, *J. Surfactants Deterg*,. **19**, 501 (2016).
14. M. C. Murguía, V. A. Vaillard, V. G. Sánchez, J. Di Conza, and R. J. Grau, Synthesis, surface-active properties, and antimicrobial activities of new double-chain gemini surfactants, *J. Oleo Sci*., **57**, 301 (2008).
15. J. Haldar, P. Kondaiah, and S. Bhattacharya, Synthesis, and antibacterial properties of novel hydrolyzable cationic amphiphiles. Incorporation of multiple head groups leads to impressive antibacterial activity, *J. Med. Chem.*, **48**, 3823 (2005).
16. P. Gilbert and L. E. Moore, Cationic antiseptics: diversity of action under a common epithet, *J. Appl Microbiol.*, **99**, 703 (2005).
17. N. Rodrigues de Almeida, Y. Han, J. Perez, S. Kirkpatrick, Y. Wang, and M. C. Sheridan, Design, synthesis, and nanostructure-dependent antibacterial activity of cationic peptide amphiphiles, *ACS Appl. Mater. Inter.*, **11**, 2790 (2018).
18. Â. S. Inácio, N. S. Domingues, A. Nunes, P. T. Martins, M. J. Moreno, L. M. Estronca, O. V. Vieira, Quaternary ammonium surfactant structure determines selective toxicity towards bacteria: mechanisms of action and clinical implications in antibacterial prophylaxis, *J. Antimicrob. Chemoth.*, **71**, 641 (2016).
19. M. N. Jones, Surfactants in membrane solubilization, *Int. J. pharmaceut*, **177**, 137 (1999).
20. J. Chen, S. Li, J. Luo, R.Wang, and W. Ding, Enhancement of the antibacterial activity of silver nanoparticles against phytopathogenic bacterium Ralstonia solanacearum by stabilization, *J. Nanomater.*, **1**, 1 (2016).